



On the hydrodynamics of bobbing cones

K.R. Drake^{a,*}, R. Eatock Taylor^b, P.H. Taylor^b, W. Bai^c

^a Department of Mechanical Engineering, University College London, Torrington Place, London WC1E 7JE, UK

^b Department of Engineering Science, University of Oxford, Parks Road, Oxford OX1 3PJ, UK

^c Department of Computing and Mathematics, Manchester Metropolitan University, Chester Street, Manchester M1 5GD, UK

ARTICLE INFO

Article history:

Received 14 October 2008

Accepted 18 July 2009

Available online 28 July 2009

Keywords:

Cone

Flared body

Transient oscillation

Relative motion

Potential flow

Setup

ABSTRACT

The paper describes an experimental investigation into the hydrodynamics of a right circular cone undergoing transient forced vertical oscillations in otherwise still water. Attention is given to the vertical fluid force and the relative vertical motion between the cone and its intersection with the adjacent free water surface. Comparisons are made between linear theory and experimental results extracted from paired response time histories obtained with input displacements of opposite sign. Comparisons are also made with the predictions obtained from fully non-linear numerical models. A slowly varying setup is observed in the measured relative vertical motion and a new second order term is identified in order to formulate a theoretical explanation.

© 2009 Elsevier Ltd. All rights reserved.

1. Introduction

The interaction between steep waves and marine structures has been the subject of much interest in recent years within the naval architecture and ocean engineering communities. Particular problems include: wave loading at the bows of FPSOs, tankers and ferries; and green water loading on FPSOs and bulk carriers.

The need to limit the green water loading on FPSOs has led to the incorporation of substantial raised forecastle and bulwark structures. Amongst typical designs are those that feature a rounded bow with pronounced flare above the still waterline. Some certification societies call for additional localised strengthening to be incorporated in FPSO vessels with a rounded bow and flare (Health and Safety Executive, 2000). At present, the basis for design guidance in this area is highly empirical. We envisage that improvements could be made in this area when suitable non-linear computational methods are developed for analysing the hydrodynamics of flared bodies.

The computation of first and second order effects in potential flow theory considers only the geometry of the body surface below the still water level, and in special cases the non-vertical slope of the body surface at the waterline. In order to address the problems of bodies where the flare extends above still water level, we consider that it will be necessary to use a fully non-linear computational method rather than a perturbation expansion about the still water level.

The experimental work reported in this paper is allied to research efforts directed towards the development of fully non-linear computational methods suitable for the sensitive problems of flared bodies. The aim has been to generate high quality data from physical experiments which feature flared geometry in order to provide simple validation cases for the developing computational methods. From this it was decided to investigate the case of a right circular cone undergoing forced vertical oscillations (i.e. bobbing) in otherwise still water. Given the development stage of the non-linear computational methods, we have chosen to concentrate upon parameters such as global forces and relative vertical motion, rather than attempting to quantify highly non-linear effects (thin jets, local wave breaking, etc.).

Unlike linear water wave problems which are solved in the frequency domain, the corresponding fully non-linear computational methods must be tackled in the time domain. When an integral equation/boundary element method is used for the linear problem it is only necessary to solve for unknowns on the body surface. This is because it is possible to employ Green's functions which satisfy the appropriate boundary conditions on the free surface, the seabed and for radiation of waves away from the body to infinity. However, the fully non-linear case requires solution for unknowns both on the free surface and the body surface. In order to reduce the computational burden, it is useful to consider synthesising short duration events that are relevant for design purposes. This has the benefit of not only limiting the extent of the computations in the time domain but also the required size of the physical domain due to the finite speed of wave propagation. With this being a likely context for the practical application of fully non-linear computational methods, it was decided that for the

* Corresponding author. Tel.: +44 207 679 3916.

E-mail address: k_drake@meng.ucl.ac.uk (K.R. Drake).

physical experiments the prescribed time histories for the vertical motion of the cone should follow the profile of a Gaussian wave packet.

Masuda et al. (1992) investigated the second order steady and double frequency force on a conical shaped floating body in regular waves. The cone angle was such that the radius increased with depth below the still water level, which is inverted compared to the case considered in this paper. The effects of cone angle on the formulation of the second order waterline forces were incorporated in the analysis and found to have a considerable influence on the results. However, the effects of body motions were neglected, this being an appropriate assumption for the towing phase associated with the installation of a large cone type concrete platform.

Attention in this paper is given to the vertical fluid force acting on the cone and also the vertical motion of the cone relative to the adjacent free water surface. Comparisons are made between experimental measurements and predictions obtained from linear and non-linear theoretical models. Particular effort has been given to formulating an explanation for the slowly varying setup that was observed in the measurement of relative vertical motion.

2. Experimental design

2.1. Oscillating cone

The cone was forced to oscillate vertically in otherwise still water in a wave tank in the Department of Mechanical Engineering at University College London. A schematic of the arrangement that was used is shown in Fig. 1. The linear motion system comprised a precision ball screw assembly driven by an AC servo motor and digital drive controller. The system was configured to move in accordance with prescribed time histories of vertical displacement.

The right circular cone was constructed from lightweight foam modelling board and was hollowed out internally to reduce weight. A coating system was applied to produce a smooth hard finish on the exterior surface. The cone was located centrally across the width of the tank. The tank width was 2.5 m and the water depth was 1.01 m. The longitudinal position of the cone was 7.77 m from the wavemaker units at one end of the tank and 9.35 m from the waterline intersection of the sloping beach at the

other end. The cone draught, which is equal to the waterline radius in case of a right circular cone, was estimated to be 148 mm (see Section 3).

2.2. Input motion

The vertical position of the cone $w(t)$ followed the form of a Gaussian wave packet defined by

$$w(t) = -A \operatorname{Re} \left\{ \sum_n \alpha_n e^{i\omega_n t} \right\}$$

$$\alpha_n = \frac{1}{\sigma \sqrt{2\pi}} e^{-((\omega_n - \omega_0)^2 / 2\sigma^2)} \Delta\omega$$

$$\sigma = \omega_0 / 2\pi \quad (1)$$

Note that upward motion is positive and $\lim_{\Delta\omega \rightarrow 0} \sum_n \alpha_n = 1$.

A positive value for A produces a time history with its largest excursion being a downward displacement $w = -A$ at time $t = 0$. The dependency in Eq. (1) of σ on the central frequency, ω_0 , was chosen to maintain the shape of the packet when frequency is varied.

2.3. Instrumentation

A 250 N load cell was fitted between the cone and the lower end of the connecting rod. Four thin plastic strips, placed horizontally at right angle intervals, were used to provide radial connections between the cone rim and a collar attached around the connecting rod. This was done as a precautionary measure to prevent the transmission of bending moments into the load cell that might be caused by accidental loads and imperfections in the symmetry of the fluid loading. The strips were stiff in tension but very flexible in bending so that the principal load path for vertical fluid forces would be through the load cell.

A twin wire wave probe was fitted adjacent to the cone surface and calibrated to give the relative vertical motion between the cone and its intersection with the free water surface. The alignment of the probe was parallel to a generator of the cone surface at a perpendicular distance of approximately 3 mm.

Three separate analogue signals were sampled using a data acquisition unit. The signals corresponded with the force from the load cell, the relative vertical motion from the twin wire probe and the vertical displacement from the linear motion system. The sampling frequency was set at 100 Hz on each channel for all of the tests.

3. Data analysis

The cone draught in the rest condition was estimated initially from direct measurement of physical dimensions. However, the precision of the measurement was limited by surface tension effects and so it was decided to adjust the estimate (by approximately 1%) to give an improved fit between the measured force and calculated quasi-static buoyancy force in slow constant speed tests. The latter involved a vertical speed of approximately 2 mm/s over the full range of travel of the linear motion system (i.e. 78 mm up and 78 mm down). This resulted in a best estimate of 148 mm for the cone draught.

The raw time histories of measured force contained response components that were at frequencies above those associated with sum frequency second order hydrodynamic forces. The observed behaviour at these frequencies was rather complex and attributed mainly to control aspects of the linear motion system and to a

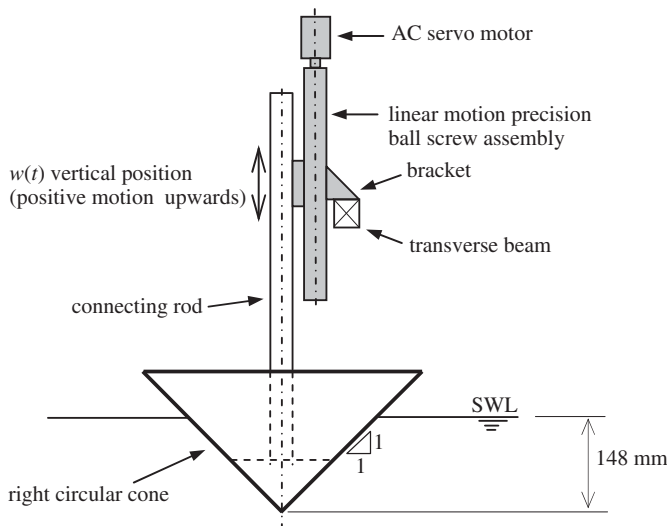


Fig. 1. Schematic showing cone and linear motion system.

lesser extent on elasticity effects in the support arrangement. Because of these findings it was deemed necessary during post-processing of the experimental data to apply low-pass digital filtering with a cut-off frequency of $3\omega_0$. This frequency is slightly above $2(\omega_0 + 3\sigma)$, thereby retaining the measurement of first and second order hydrodynamic forces associated with the Gaussian wave packet. The drawback is the exclusion of some possible third order effects from the data analysis. In contrast with the force signal, the relative vertical motion exhibited minimal signal levels at frequencies above $3\omega_0$. The signal for the actual displacement of linear motion system was typically within 1 mm of the demanded signal throughout its operation.

It was necessary to correct for inertial effects associated with the dry mass of the cone and fittings in order to produce time histories of the measured fluid force. The displacement signal was twice differentiated to give acceleration time histories and then combined with the dry mass of 1.356 kg to produce time histories of the D'Alembert inertial force. The latter was then applied to the load cell measurements to produce time histories of fluid forces.

Separate tests were carried out with positive and negative values for the largest excursion from the rest position. The purpose was to provide a basis for the subsequent extraction of odd and even order components from the hydrodynamic responses during the post-processing of experimental data. The underlying principle is that odd orders change sign when the sign for A in Eq. (1) is reversed whilst even orders remain the same.

For a system with only linear and quadratic non-linear behaviour, the first order component of measured force $F_1(t)$, for example, can be extracted by evaluating the half-difference of the measured time histories from two tests, thus

$$F_1(t) = \frac{1}{2} \{ F^{A+}(t) - F^{A-}(t) \} \quad (2)$$

and the second order component $F_2(t)$ of measured force can be extracted from the half-sum, thus

$$F_2(t) = \frac{1}{2} \{ F^{A+}(t) + F^{A-}(t) \} \quad (3)$$

where $F^{A+}(t)$ and $F^{A-}(t)$ denote the measured time histories of total force obtained in separate tests which are identical in all respects apart from the sign of the value for A . This process was applied to the filtered time histories of both measured force and relative vertical motion.

4. Theoretical models

4.1. Linear

When the vertical oscillations of the cone are small compared to its draught, it is appropriate to assume that the prediction of hydrodynamic responses can be based on the assumption of linear irrotational flow for an incompressible inviscid fluid (i.e. potential flow). Superposition may be applied to the frequency components in the Gaussian packet, defined in Eq. (1), to give the corresponding linear prediction of the vertical component of the total fluid loading acting on the cone

$$F_1(t) = A \operatorname{Re} \left\{ \sum_n (-\omega^2 a_{33} + i\omega b_{33} + \rho g \pi c^2) \alpha_n e^{i\omega_n t} \right\} + \frac{1}{3} \rho g \pi c^3 \quad (4)$$

where a_{33} and b_{33} are the frequency dependent heave added mass and damping, c the waterline radius (equal to the draught for a right circular cone), ρ the fluid density and g the acceleration due

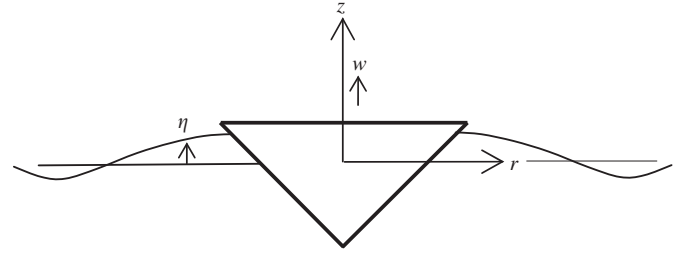


Fig. 2. Fixed coordinate system, cone position and free surface elevation.

to gravity. Upward forces are positive. Note that Eq. (4) incorporates both hydrodynamic and hydrostatic loading.

The first order relative vertical motion ξ_1 between the cone and its intersection with the free water surface is given by

$$\xi_1 = \eta_1 - w \quad (5)$$

where η_1 is the first order free surface elevation relative to still water level, and w the vertical displacement of the cone. The first order free surface elevation is given by

$$\eta_1 = - \frac{1}{g} \frac{\partial \Phi_1}{\partial t} \Big|_{z=0} \quad (6)$$

where Φ_1 is the first order velocity potential. Fig. 2 shows the fixed coordinate system, cone position and free surface elevation. The first order free surface elevation in Eq. (6) is evaluated at the intersection between still water level and the cone at its rest position (i.e. at $r = c$).

It is appropriate to consider the evaluation of hydrodynamic response for the case when the fluid is unbounded in the horizontal directions. For a right circular cone undergoing heave oscillations, the flow field will then exhibit axial symmetry about its vertical axis of revolution. Such an approach ignores effects associated with the finite width and length of the tank.

Eatock Taylor and Dolla (1979) described the application of a boundary integral method and computer program for the computation of linear hydrodynamic loading on vertical bodies of revolution undergoing motion in regular waves. A Fourier series was applied to the velocity potential in the direction of the azimuth angle thereby enabling surface integrals to be reduced to line integrals. For the heave oscillations of such bodies in otherwise still water the velocity potential for the flow field is represented solely by the first term (i.e. zeroth harmonic) of the Fourier series. This program has been used for generating the linear results presented in this paper.

4.2. Non-linear force under slowly varying input motion

Here we make the approximation that the hydrodynamic pressure is uniform over the immersed surface of the cone and note that pressure is constant on the free water surface. This means that the corresponding estimate of total fluid pressure will increase linearly, from atmospheric pressure, with increasing depth below the instantaneous elevation of the free water surface. The vertical component of fluid loading can then be estimated from the instantaneous buoyancy force calculated in a quasi-static manner, thus

$$F = \frac{1}{3} \rho g \pi (\xi_1 + c)^3 \quad (7)$$

where $\xi_1 + c$ represents the instantaneous draught of the cone.

4.3. Second order slowly varying component of relative vertical motion

Here we consider two components: the first η_2 being the second order wave surface elevation at $r = c$, and the second being a new term which accounts for the horizontal shift in the intersection of the free water surface with the cone. The total second order relative vertical motion ξ_2 is given by

$$\xi_2 = \eta_2 + (\eta_1 - w) \frac{\partial \eta_1}{\partial r} \quad (8)$$

The second order wave surface elevation (e.g. Sarpkaya and Isaacson, 1981) is given by

$$\eta_2 = -\frac{1}{g} \left[\eta_1 \frac{\partial^2 \Phi_1}{\partial z \partial t} + \frac{1}{2} |\nabla \Phi_1|^2 + \frac{\partial \Phi_2}{\partial t} \right]_{z=0} \quad (9)$$

Noting that on $z = 0$ we have

$$\frac{\partial \Phi_1}{\partial z} = \frac{\partial \eta_1}{\partial t} \quad (10)$$

and considering regular oscillation at frequency ω so that

$$\eta_1 = \text{Re}\{\zeta_1 e^{i\omega t}\}, \Phi_1 = \text{Re}\{\phi_1 e^{i\omega t}\} \quad (11)$$

we obtain the mean second order wave surface elevation as

$$\overline{\eta_2} = -\frac{1}{2g} [-\omega^2 |\zeta_1|^2 + \frac{1}{2} |\nabla \phi_1|^2]_{z=0} \quad (12)$$

where it is noted that the second order velocity potential does not contribute to the mean wave surface elevation.

Consider, however, the term $\nabla \Phi_1$ in Eq. (9), the velocity of a fluid particle on the waterline. Because of axisymmetry there is no dependency on the azimuth angle. The other components are easily found in terms of $\partial \eta_1 / \partial t$ and $\partial w / \partial t$. In Fig. 3, the solid arrow is the velocity vector of the cone, and open arrows are components of velocity of a fluid particle on the cone surface at the waterline. The velocity of the fluid along the cone generator is unknown, but we know the vertical component is $\partial \eta_1 / \partial t$. Hence we see for a right circular cone that $\partial \Phi_1 / \partial r = \partial \eta_1 / \partial t - \partial w / \partial t$, so

$$\frac{1}{2} |\nabla \Phi_1|^2 = \frac{1}{2} \left(\frac{\partial \eta_1}{\partial t} \right)^2 + \frac{1}{2} \left(\frac{\partial \eta_1}{\partial t} - \frac{\partial w}{\partial t} \right)^2 = \left(\frac{\partial \eta_1}{\partial t} \right)^2 - \frac{\partial w}{\partial t} \left(\frac{\partial \eta_1}{\partial t} - \frac{\partial w}{\partial t} \right) - \frac{1}{2} \left(\frac{\partial w}{\partial t} \right)^2 \quad (13)$$

Letting $w = \text{Re}\{\alpha e^{i\omega t}\}$ and returning to Eq. (12) we obtain

$$\overline{\eta_2} = \frac{\omega^2}{2g} \text{Re} \left\{ \zeta_1 \alpha - \frac{\alpha^2}{2} \right\} \quad (14)$$

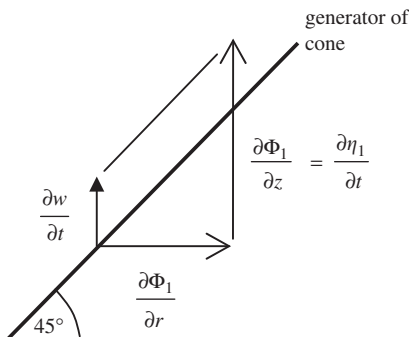


Fig. 3. Cone and fluid particle velocity components at the waterline.

Now we consider the evaluation of the new term associated with the horizontal shift of the intersection of the free water surface with the cone. First we consider the slope of the water surface in the radial direction

$$\begin{aligned} \frac{\partial \eta_1}{\partial r} &= -\frac{1}{g} \frac{\partial^2 \Phi_1}{\partial r \partial t} \Big|_{z=0} = -\frac{1}{g} \frac{\partial}{\partial t} \left(\frac{\partial \eta_1}{\partial t} - \frac{\partial w}{\partial t} \right) \\ &= -\frac{1}{g} \left(\frac{\partial^2 \eta_1}{\partial t^2} - \frac{\partial^2 w}{\partial t^2} \right) \end{aligned} \quad (15)$$

and then obtain the change in free surface elevation by multiplying the slope by the horizontal shift of the free water surface intersection with the cone, thus

$$\begin{aligned} (\eta_1 - w) \frac{\partial \eta_1}{\partial r} &= -\frac{1}{g} (\eta_1 - w) \left(\frac{\partial^2 \eta_1}{\partial t^2} - \frac{\partial^2 w}{\partial t^2} \right) \\ &= \frac{1}{g} \left(-\eta_1 \frac{\partial^2 \eta_1}{\partial t^2} + \eta_1 \frac{\partial^2 w}{\partial t^2} + w \frac{\partial^2 \eta_1}{\partial t^2} - w \frac{\partial^2 w}{\partial t^2} \right) \end{aligned} \quad (16)$$

The mean value of this component is given by

$$(\eta_1 - w) \frac{\partial \eta_1}{\partial r} = \frac{\omega^2}{2g} \text{Re} \{ \zeta_1 \zeta_1^* - 2\zeta_1 \alpha + \alpha^2 \} \quad (17)$$

where the superscript asterisk denotes the complex conjugate. Combining Eqs. (14) and (17) we obtain the mean vertical relative motion in regular oscillations as

$$\overline{\xi_2} = \frac{\omega^2}{2g} \text{Re} \left\{ \frac{1}{2} \alpha^2 - \zeta_1 \alpha + \zeta_1 \zeta_1^* \right\} \quad (18)$$

This can be expressed in non-dimensional form as

$$\frac{\overline{\xi_2}}{\alpha} = \frac{\omega^2 \alpha}{2g} \text{Re} \left\{ \frac{1}{2} - \frac{\zeta_1}{\alpha} + \frac{\zeta_1 \zeta_1^*}{\alpha^2} \right\} = \alpha Q(\omega) \quad (19)$$

where $Q(\omega)$ is the quadratic transfer function of relative vertical motion on the cone given by

$$Q(\omega) = \frac{\omega^2}{2g} \text{Re} \left\{ \frac{1}{2} - Z_1 + Z_1 Z_1^* \right\} \quad (20)$$

and Z_1 denotes the linear transfer function of relative vertical motion.

The analysis may be extended to the Gaussian packet in Eq. (1) if we use the equivalent of the Newman approximation (Newman, 1975), the latter being commonly used for the estimation of slowly varying drift forces for moored vessels. If we consider the packet in Eq. (1), the non-dimensional slowly varying component of relative motion (i.e. component associated with difference frequencies) can be written in the form

$$\frac{\xi_2(t)}{A} \approx A \sum_m \sum_n \left\{ \alpha_m \alpha_n \frac{1}{2} (Q_m + Q_n) e^{i(\omega_m - \omega_n)t} \right\} \quad (21)$$

where $Q_m = Q(\omega_m)$ and $Q_n = Q(\omega_n)$. Thus the quadratic transfer function in bichromatic oscillations has been estimated from the average of the quadratic transfer for regular oscillations at frequencies ω_m and ω_n .

4.4. Fully non-linear

The experiments described here aimed to provide a dataset of hydrodynamic results for a flared body, such as could contribute to the validation of fully non-linear numerical models. One such model, with which comparisons are given below, has been presented by Bai and Eatock Taylor (2006, 2007). Like the linear and second order approaches above, it is based on the

assumptions of potential flow theory; but it models the full non-linear free surface conditions, and the Neumann boundary condition on the actual position of the moving body. The numerical representation uses a boundary element approach, with quadratic isoparametric triangular and quadrilateral elements. This facilitates meshing of the free surface or body boundaries (as compared with, say, volume-discretised approaches). Such remeshing at frequent time intervals is important in case of large free surface motions, and for bodies with pronounced flare or undergoing large (especially rotational) displacements. Details of the numerical approach and meshing, including issues of convergence and validation, are given in Bai and Eatock Taylor (2006, 2007).

The boundary motions are tracked in discrete time using the mixed Eulerian–Lagrangian technique. The free surface elevation at the body waterline (for which results are given below) results directly from this tracking, coupled with a technique to force the relevant free surface nodes to remain on the body surface. The relative motion between cone and free surface is measured in the experiments. The corresponding numerical prediction is obtained simply by subtracting the prescribed cone motion from the computed free surface motion. The velocities of the meshed surfaces are obtained from the nodal potentials using the gradients of the quadratic shape functions, in association with the known normal derivatives of the potential on the surface. The forces on the body are calculated using auxiliary functions, as described by Wu and Eatock Taylor (2003). This approach has the advantage of avoiding simple time-differencing to obtain the contribution of $\partial\Phi/\partial t$ to the pressure; thereby problems of inaccuracy and, at worst, instability may be overcome.

For the fully non-linear results given below, the cone is modelled in a circular tank with a diameter of 2.5 m for all of the cases. This corresponds to the width of the rectangular tank used for the experiments, and provides a convenient way of representing some effects due to side wall reflections, such as was observed at the later stages in some of the experiments. The assessment of such reflections using the linear theory has been reported in Eatock Taylor et al. (2009), where it is shown that for the cases considered here in a circular tank the linear theory predicts no discernible effects of reflections until well after the time at which the cone has its peak displacement.

5. Results

The force measurements have been adjusted to give a datum of zero for the case when the cone and water surface are at rest. The force results have been expressed in non-dimensional form as $F/\rho g \pi c^2 |A|$ where F is the time varying component of the vertical fluid force. In the plotted results, time has been expressed in non-dimensional form by dividing through by the period $T_0 = 2\pi/\omega_0$ that corresponds with the central frequency of the Gaussian packet. Relative vertical motion has been expressed in non-dimensional form as $\xi/|A|$.

Fig. 4 shows the measured and predicted time histories of vertical force for the case of slowly varying input motion when $\omega_0^2 c/g = 0.149$ and $A/c = 0.338$ (i.e. a Gaussian packet with a central frequency of 3.142 rad/s and a maximum downward excursion of 50 mm). The predicted values are based upon Eq. (7) which involves a quasi-static calculation of the buoyancy force taking into account the effect of first order relative vertical motion between the cone and the adjacent free water. The agreement between the results is very good throughout the entire duration of the Gaussian packet. The importance of accounting for the motion of the free surface becomes apparent when the non-dimensional relative vertical motion in Fig. 5 is considered. The

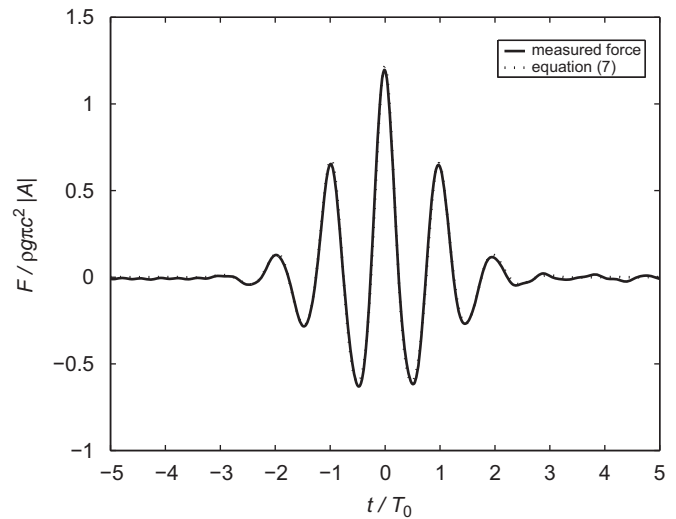


Fig. 4. Comparison between measured and predicted total force for the case of slowly varying input motion when $\omega_0^2 c/g = 0.149$ and $A/c = 0.338$.

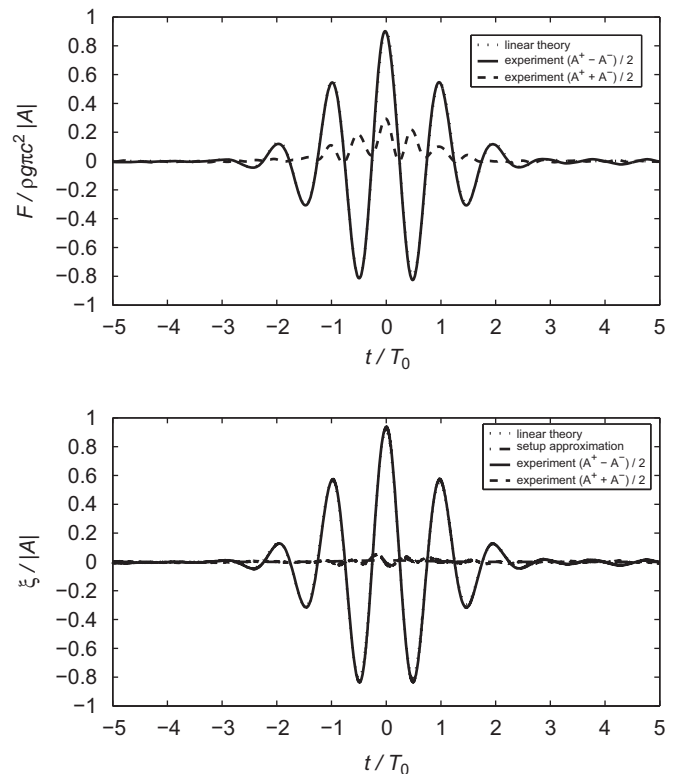


Fig. 5. Comparison between theoretical predictions and combined experimental results when $\omega_0^2 c/g = 0.149$ and $A/c = \pm 0.338$.

maximum relative vertical motion from the linear theory is approximately 9% lower than the corresponding absolute excursion of the cone from still water level. This is particularly significant given the cubic relationship between the instantaneous draught and the quasi-static buoyancy force in Eq. (7).

Figs. 5–8 inclusive provide comparisons between theoretical predictions and combined experimental results when $A/c = \pm 0.338$ for four different values of central frequency. The experimental results for each central frequency have been combined to give the half-difference and half-sum of the time

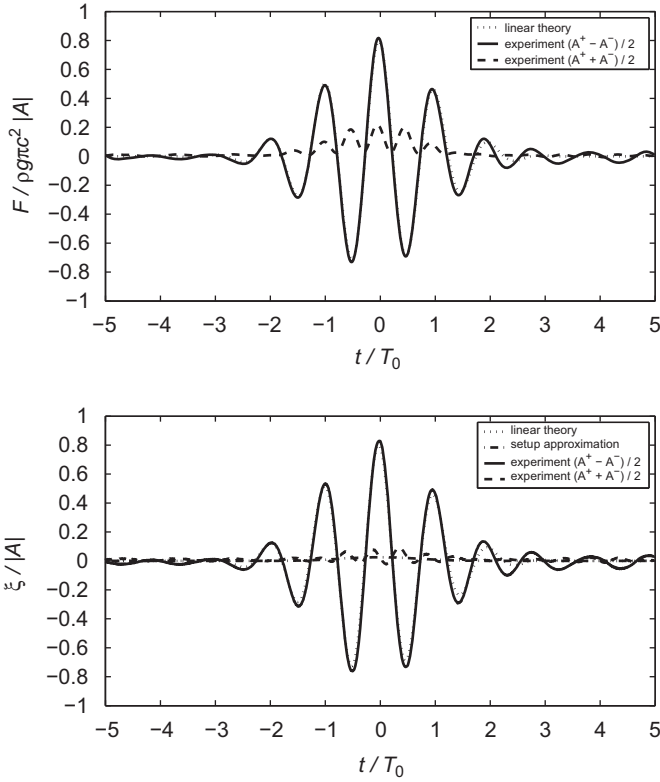


Fig. 6. Comparison between theoretical predictions and combined experimental results when $\omega_0^2 c/g = 0.414$ and $A/c = \pm 0.338$.

histories obtained for negative and positive Gaussian packets, these being denoted respectively as $(A^+ - A^-)/2$ and $(A^+ + A^-)/2$ in the legends. The same process has been applied to the time histories of vertical force and relative vertical motion. The agreement between linear theory and the half-difference time histories is very good for most of the duration of the Gaussian packets. It should be noted that the results from the linear theory are representative of conditions away from the body in which the fluid domain is unbounded in the horizontal direction (i.e. open sea conditions). The experimental results in Figs. 6–8 clearly contain effects of reflections from the tank side walls and this is particularly noticeable when $t/T_0 > 3$. However, the agreement between open sea calculations and the half-difference time histories is generally excellent for the initial and central parts of the Gaussian packet.

The half-sum time histories for the measurement of vertical force exhibit largest peak magnitudes when $\omega_0^2 c/g = 0.149$ as shown in Fig. 5. It has been demonstrated in Fig. 4 that the vertical forces at such frequencies can be predicted with good accuracy using the approximation given by Eq. (7). The magnitudes of the vertical force peaks appear to reduce with increasing central frequency, as shown by the progression from Figs. 5–8, and most notably this seems to be associated with a reduction in the magnitudes of the higher frequency components which are associated with second order sum frequencies.

The half-sum time histories for the measurement of relative vertical motion have their lowest magnitude peaks when the central frequency is lowest. However, as the central frequency increases there is a general increase in the levels of relative vertical motion and this is most evident in the slowly varying component that appears in Fig. 8. We refer to this effect as a setup in the relative vertical motion. It is evident that the approximate method described in Section 4.3 appears to provide a very good basis for estimating its magnitude.

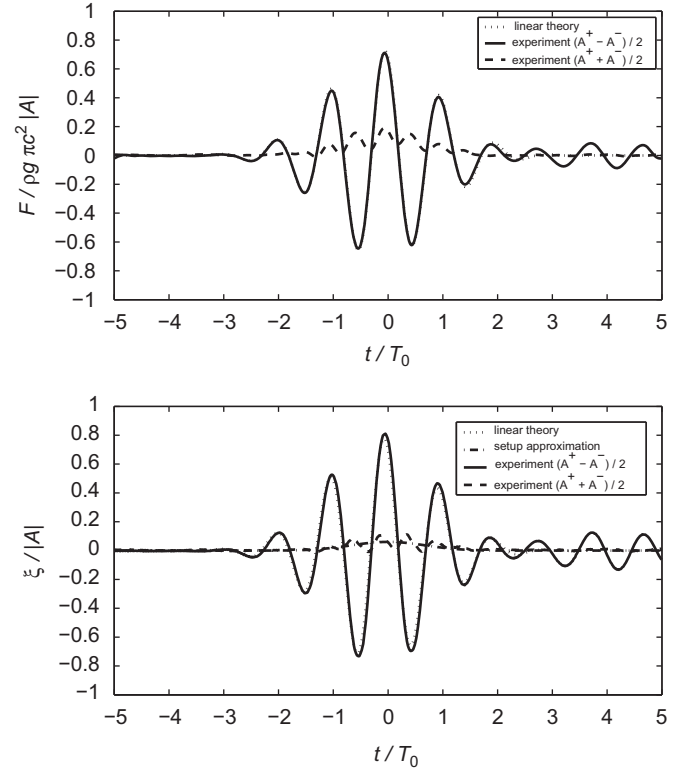


Fig. 7. Comparison between theoretical predictions and combined experimental results when $\omega_0^2 c/g = 0.811$ and $A/c = \pm 0.338$.

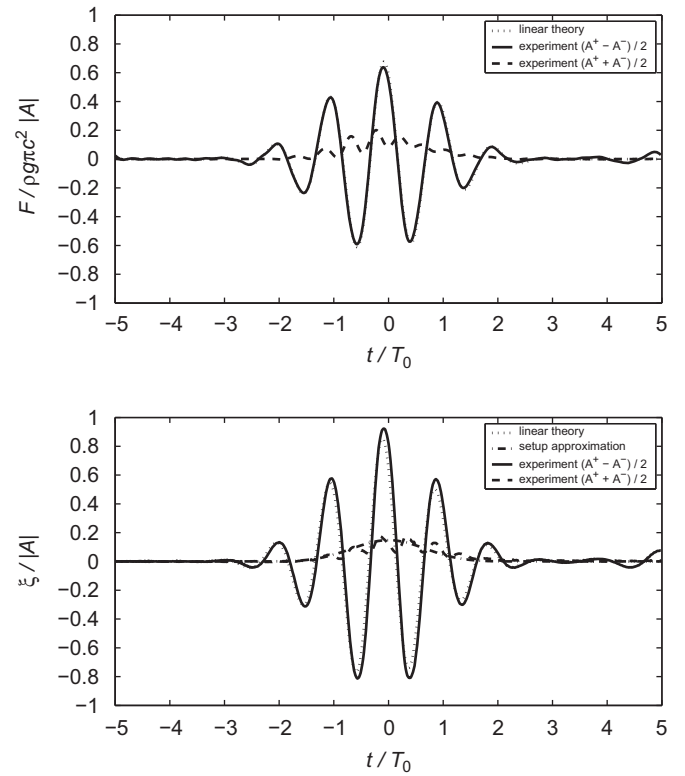


Fig. 8. Comparison between theoretical predictions and combined experimental results when $\omega_0^2 c/g = 1.34$ and $A/c = \pm 0.338$.

Figs. 9 and 10 show comparisons of the linear and fully non-linear simulations with the experimental results, for two of the central frequencies in the middle of the range considered in

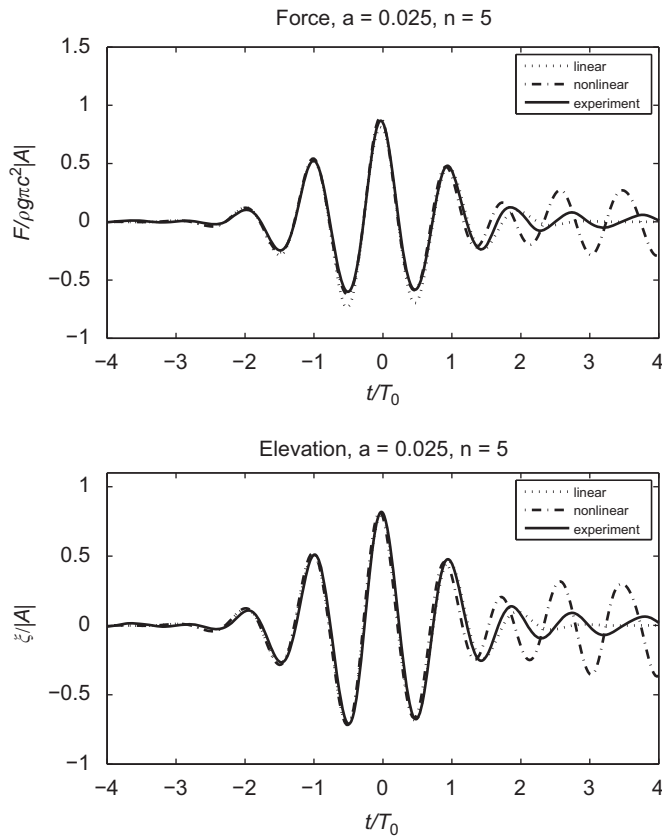


Fig. 9. Comparisons of linear and non-linear simulations with experimental results when $\omega_0^2 c/g = 0.414$ and $A/c = +0.169$.

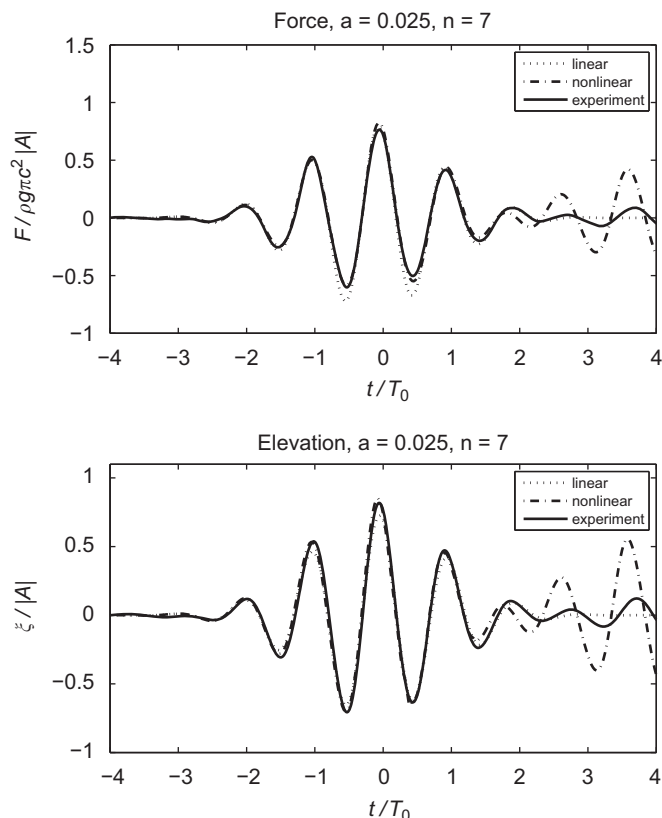


Fig. 10. Comparisons of linear and non-linear simulations with experimental results when $\omega_0^2 c/g = 0.811$ and $A/c = +0.169$.

Figs. 5–8. These correspond to the imposed motions with positive Gaussian packets at $A/c = 0.169$: this amplitude was also tested in the experiments for the same central frequencies, and it was these cases for which some comparisons have been made with the non-linear boundary element method theory. For each central frequency, plots of non-dimensionalised force F and relative vertical motion ξ have been obtained. The latter is measured directly in the experiment, whereas the direct output from the theoretical simulations is the absolute elevation. They are of course simply related by Eq. (5). It may be noted that the effects of reflections are evident in both the experimental data and in the numerical results during the later stages of the records for these cases. Not surprisingly these are larger for the simulations in a circular tank than for the experimental data in a long rectangular tank of the equivalent width. It is shown in Eatock Taylor et al. (2009) that a linear analysis of the problem which is analysed here by a fully non-linear simulation leads to reflected waves which are very similar. The relative importance of these waves appears to be strongly linked to the relationship of the peak period of the prescribed motion packet to the natural frequencies of standing waves in the tank.

Considering first the comparisons of forces F , we see that in each case the non-linear simulations are much closer to the experimental results than to the predictions from linear theory. Both the non-linear simulations and experimental results show clear evidence of steepening of the crest and flattening of the two troughs on either side of the force time histories, as compared with linear theory. In the results for the relative free surface displacement ξ , the non-linear simulations are also considerably better than the linear theory at predicting the experimental behaviour. The results for the other central frequencies (not included here) further support these remarks. Generally the non-linear simulations appear satisfactory when presented in this manner.

6. Conclusions

Experiments involving the transient forced vertical oscillation of a right circular cone have been undertaken. The use of paired response time histories with opposite sign for the prescribed input displacement has enabled successful comparisons to be made with predictions obtained from the linear theory. It is also evident that the experimental results provide a useful basis for validation of fully non-linear numerical models, as used to analyse the sensitive problem of flared bodies. This has been illustrated here by comparison of the experimental time histories with some preliminary results from one such non-linear model based on the boundary element method. A significant experimental finding has been the observation of a slowly varying setup in the measured relative vertical motion. A new second order term related to the geometry of the cone has been identified, in order to formulate an explanation for the observation. The term involves a partial derivative of the first order free surface elevation with respect to the horizontal radial direction and is a feature of bodies with flared geometry at the waterline.

Acknowledgements

This work was supported by the Engineering and Physical Sciences Research Council through Grants GR/S56917 at Oxford University and GR/S56900 at University College London.

References

- Bai, W., Eatock Taylor, R., 2006. Higher-order boundary element simulation of fully nonlinear wave radiation by oscillating vertical cylinders. *Applied Ocean Research* 28, 247–265.

- Bai, W., Eatock Taylor, R., 2007. Numerical simulation of fully nonlinear regular and focused wave diffraction around a vertical cylinder using domain decomposition. *Applied Ocean Research* 29, 55–71.
- Eatock Taylor, R., Dolla, J.P., 1979. Hydrodynamic loads on vertical bodies of revolution. *Transactions of the Royal Institution of Naval Architects* 122, 285–297.
- Eatock Taylor, R., Taylor, P. H., Drake, K.R., 2009. Tank wall reflections in transient testing. 24th International workshop on Water Waves and Floating Bodies, Zelenogorsk, 19–22 April.
- Health and Safety Executive, 2000. Offshore Technology Report—OTO 2000 004. Review of greenwater and wave slam design and specification requirements for FPSO/FSU's. Prepared by PAFA Consulting Engineers Ltd.
- Masuda, K., Nagai, T., Shibayama, T., 1992. Second-order wave loads on cone shaped floating bodies: effect of cross angle of body and water surface. In: *Proceedings of the 11th International Conference on Offshore Mechanics and Arctic Engineering*, vol. 1-A, pp. 105–116.
- Newman, J.N., 1975. Second-order, slowly-varying forces on vessels in irregular waves. In: Bishop, R.E.D., Price, W.G. (Eds.), *Proceedings of International Symposium on the Dynamics of Marine Vehicles and Structures in Waves*. University College London, Institution of Mechanical Engineers, London, pp. 182–186.
- Sarpkaya, T., Isaacson, M., 1981. *Mechanics of wave forces on offshore structures*. Van Nostrand Reinhold, ISBN: 0-442-25402-4, p. 170.
- Wu, G.X., Eatock Taylor, R., 2003. The coupled finite element and boundary element analysis of nonlinear interactions between waves and bodies. *Ocean Engineering* 30, 387–400.